Regular Article

The role of disorder in the domain wall dynamics of magnetic nanostrips[*]

Ben Van de Wiele[1,a], Lasse Laurson[2,b], and Gianfranco Durin[3,4,c]

[1] Department of Electrical Energy, Systems and Automation, Ghent University, 9000 Ghent, Belgium
[2] COMP Centre of Excellence, Department of Applied Physics, Aalto University, P.O. Box 14100, 00076 Aalto, Finland
[3] ISI Foundation, Via Alassio 11/c, 10126 Torino, Italy
[4] Istituto Nazionale di Ricerca Metrologica, Strada delle Cacce 91, 10135 Torino, Italy

Abstract. We study the role of the disorder in the dynamics of the domain walls (DW) in nanostrips with in-plane magnetization. In contrast with previous works where the disorder is due to edge roughness, we consider the role of a random distribution of voids, thus simulating local changes of the magnetization saturation value. By making use of the high-speed computational capability of GPUs, and an ad hoc micromagnetic code, we compute the speed of DWs under both applied fields (up to 15 mT), and spin-polarized currents (up to 30 A/μm^2), for four different void densities. Field and currents are applied for 20 ns. We also consider both adiabatic and non-adiabatic spin-torque effects (ξ parameter equal 0 and 0.04, respectively). For all the cases, we repeat the simulation for 50 realizations of the void distributions. No thermal effects are considered. While some results can be understood in the line of the models reported in the literature, some others are much more peculiar. For instance, we expect a lower value of the maximum DW speed. This actually occurs in the field driven case, but with a less dramatic drop at the Walker breakdown, due to the difficulty to nucleate an antivortex DW. When nucleated, it gets easily pinned, thus preventing its retrograde motion typical for disorder-free strips. In the case of current drive with non-adiabatic spin-transfer torque, the Walker breakdown current increases strongly with the void density. This results in an increased value of the maximum speed available. Another important consequence of the disorder is that at low fields/currents the depinning transition regions appear to be more rounded, resembling creep behavior. This can have important consequences in the interpretation of experimental data.

1 Introduction

A very promising set of future spintronics devices is based on the static and dynamical properties of the domain walls (DWs), as non-volatile memories [1,2], nano-oscillators [3–5], logic devices [6,7], and as sensors and amplifiers [8]. The possibility to apply spin-polarized currents to manipulate the DW position and dynamics through the spin-transfer torque (STT) mechanisms opened to a large set of studies firstly focused on in-plane magnetization nanostrips (mostly based on permalloy), and progressively moved to out-of-plane magnetization media (with high perpendicular magnetic anisotropy such as CoPt), which require lower applied currents, thanks to the enhanced non-adiabatic STT [9]. In all these devices it is fundamental to fully control the DW position and motion, and

limiting all the spurious effects, such as thermal fluctuations and any structural disorder. To control the DW position, many solutions have been proposed, mostly based on geometrical constrictions (artificial notches, etc.), that act as pinning potentials for the walls. To unpin the DWs, the power consumption (i.e. the required amplitude of spin-polarized currents) must be reduced as much as possible to limit the Joule-heating. But, at the same time, the currents must be large enough to reach the highest DW speed, so to have ultrafast non-volatile devices required by the future spintronics applications and by the market.

To understand and control any spurious effect is also mandatory for any reproducible and reliable device. Thermal effects are important especially when they are able to overcome the DW pinning potential. In case of relevant Joule heating effects due to high current densities, it is also possible to have changes of the magnetization saturation, especially approaching the Curie temperature. In general, thermal effects can highly influence the DW motion, acting as a stochastic random magnetic field, or activating the DW depinning, resulting in a creep-like curve of the DW speed at low fields/currents, below their deterministic depinning threshold (see Ref. [10] for a review).

---

[a] e-mail: ben.vandewiele@ugent.be
[b] e-mail: lasse.laurson@aalto.fi
[c] e-mail: g.durin@inrim.it

Disorder effects are much less understood. It is well known that in a disordered system, DW dynamics can be unpredictable, jerky and stochastic, as in the Barkhausen effect in higher-dimensional systems [11]. Experimental examples in nanostructures have been already reported extensively [12,13]. It is otherwise fundamental to understand and limit this intrinsic stochasticity, as any real system shows a certain degree of randomness which is reflected in the observed DW dynamics. At the same time it is in principle possible to use some form of "artificial" disorder to engineer regions of the system which can replace the geometrical constraints as reproducible pinning centers. For instance, Basith et al. [14] have recently created non-topographic regions with ion irradiation in a focused ion bean. Other studies have clearly showed that the roughness of the strip edges enhances the DW propagation [9,15], and that spatial variations of the saturation magnetization act as an increased effective damping in the dynamics of a vortex wall [16]. Also, a simplified line-based model of a transverse wall interacting with point-like, randomly distributed disorder has been presented [17,18].

In this paper, we extend our previous work [19], with the aim to study the DW dynamics with in-plane magnetization in which the source of disorder is due to a random distribution of small voids in a nanostrip. This simulates local changes of the magnetization saturation value, as for instance due to the presence of defects or/and small impurities. As expected, we found that in general the DW dynamics is (negatively) influenced by the presence of the disorder, as for instance in decreasing the maximum speed available. Remarkably, in some cases we found that the disorder is able to suppress the retrograde motion of the DW resulting in a *higher* speed. We also found that in more general terms, the curves of the DW speed vs applied/currents are significantly affected, suggesting to use caution in the interpretation of the experimental curves.

2 Micromagnetic simulations

2.1 The Landau-Lifshitz equation

As a first test to analyze the influence of disorder in the DW dynamics, we simulate a permalloy nanostrip with in-plane magnetization pointing along the strip longitudinal axis. Choosing a small thickness of 10 nm, and a width of 100 nm, DW structure is basically given by a transverse V-shape DW (V-DW), separating head-to-head domains. The time evolution of the magnetization $\mathbf{M}(\mathbf{r}, t) = M_s \hat{\mathbf{M}}(\mathbf{r}, t)$, is studied using the Landau-Lifshitz (LL) equation with the spin-transfer torque terms [20],

$$
\begin{aligned}
\frac{\partial \mathbf{M}}{\partial t} = & -\frac{\gamma}{1+\alpha^2} \mathbf{M} \times \mathbf{H}_{\text{eff}} \\
& -\frac{\alpha \gamma}{M_s(1+\alpha^2)} \mathbf{M} \times (\mathbf{M} \times \mathbf{H}_{\text{eff}}) \\
& -\frac{b_j}{M_s^2(1+\alpha^2)} \mathbf{M} \times (\mathbf{M} \times (\mathbf{j} \cdot \nabla)\mathbf{M}) \\
& -\frac{b_j}{M_s(1+\alpha^2)} (\xi - \alpha) \mathbf{M} \times (\mathbf{j} \cdot \nabla)\mathbf{M},
\end{aligned} \quad (1)
$$

where $\mathbf{H}_{\text{eff}}$ is the effective magnetic field (with contributions from the external, exchange, demagnetization), γ is the gyromagnetic ratio, α is the Gilbert damping constant, ξ is the degree of non-adiabaticity, $\mathbf{j}$ is the current density, and $b_j = P\mu_{\text{B}}/(eM_s(1+\xi^2))$, with P the polarization, μ_{B} the Bohr magneton and e the electron charge. We use the material parameters $M_s = 860 \times 10^3$ A/m and $\alpha = 0.02$.

To properly distinguish between spurious effects due to disorder and thermal fluctuations, we explicitly set the temperature to zero. The quenched disorder is simulated by introducing void cells with zero magnetization of sizes $3.125 \times 3.125 \times 10$ nm^3 at four different densities $\sigma = 3125$ μm^{-2}, 6250 μm^{-2}, 9375 μm^{-2} and $12\,500$ μm^{-2}, respectively. For each density, we make 50 realizations of the disorder.

2.2 GPU based micromagnetic simulations

We simulate equation (1) with the micromagnetic code MuMax [21] running on Graphics Processing Units (GPUs). This hardware was originally designed for image rendering but is also very suitable for high performance numerical computations. Indeed, while a CPU can only run 1 process at the time, GPUs have $\mathcal{O}(10,000)$ threads which can run in parallel. Furthermore, they have their own on-board memory which enables fast read and write operations. Therefore, in MuMax, all computations are performed on the GPU based on the instructions dictated by the CPU. This way, the much slower communication of large data sets between the CPU and GPU is minimized.

The micromagnetic computations are performed adopting a finite difference time domain discretization of the LL-equation (1). This means that the geometry is discretized using identical rectangular prisms in which the material properties as well as the fields are defined. This uniform grid enables the use of fast Fourier transform to speed up the demagnetizing field computations which is, due to their long range nature, the most time consuming part in micromagnetic simulations [22]. Furthermore, the time evolution of the magnetization is computed using Runge-Kutta time stepping schemes. The implementation of highly efficient algorithms combined with the huge parallel power of the GPU hardware makes it possible to speed up micromagnetic computations with two orders of magnitude [21]. This enables us to simulate in a reasonable time a large number of applied fields (0.5–15 mT) and currents (1–30 A/μm^2), both in the adiabatic ($\xi = 0$), and non-adiabatic case ($\xi = 0.04$).

2.3 Definition of DW speed

In a perfect system, the definition of speed of a moving wall does not represent any difficulty. One can consider the displacement traveled along a given time, and the ratio of the two quantities gives the DW speed. In the case of a disordered system, where the probability of being pinned by a random configuration of voids is not-null, we need to properly set an operative definition of the speed.
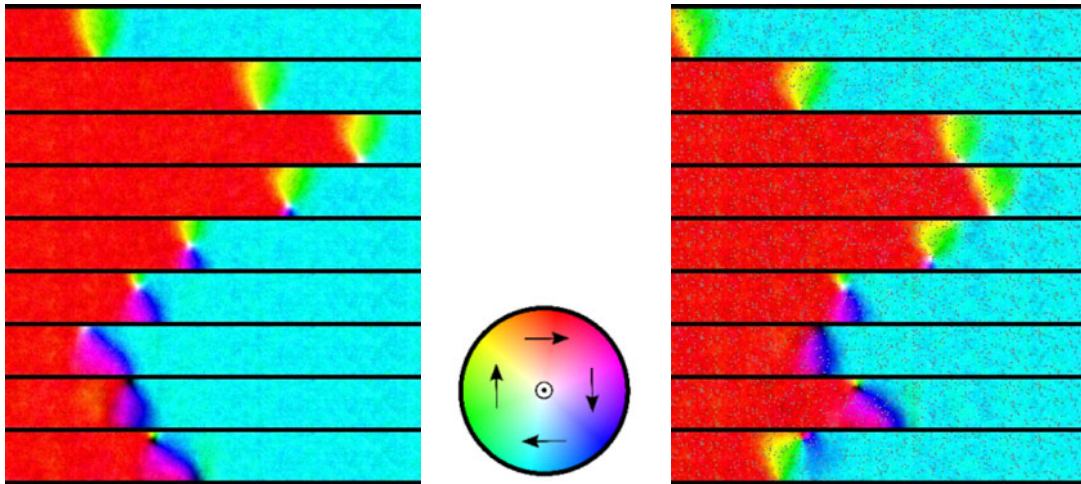
Fig. 1. (Color online) Snapshots of DW position at about 2 ns for nine applied fields (0.5, 2, 3.5, 4.5, 6.5, 8.5, 10.5, 12.5, 14.5 mT, from top to bottom, respectively), in a perfect nanostrip (left) and in a disordered nanostrip (right), having a void density of $\sigma = 6250 \ \mu\mathrm{m}^{-2}$. Sections of the strips have sizes of $100 \times 900 \ \mathrm{nm}^2$. The central core of the antivortex points upward (white) when moving from bottom to top, and downward (black) when moving from top to bottom.

To avoid fluctuations due to any transient, it is first necessary to define a starting and an ending point in the nanostrips at a given distance over which to calculate the speed. Then we can let the system run for a fixed time: we choose for instance the value $\Delta T = 20$ ns. Because of the not-null probability of pinning, we can first consider a "conditional velocity", given by DWs which actually move between the points, and get rid of any other which do not reach the second point. Except for small effects due to numerical noise, there is no possibility for the DW to depin, as we explicitly do not have any temperature effect. The DW speed is thus defined averaging over the realizations of the disorder. This definition of the DW speed is useful for a direct comparison with the void-free case, as for instance to understand the effect of the disorder to affect the maximum speed at the Walker breakdown.

On the other hand, this definition does not take into account the probability of pinning, so it is not suitable for a direct comparison with the experimental data. Thus we define an "experimental velocity" v_{exp} as the conditional velocity times the probability to reach the end, i.e. to not be pinned by the disorder. This probability actually depends on the observation time, and on the distance traveled, so v_{exp} is a scale-dependent quantity.

3 Field driven DW dynamics

3.1 Walker breakdown and collective pinning

Figure 1 shows a direct visual comparison of the different behavior of the DW dynamics in a perfect and a disordered nanostrip (at a density of 6250 void cells/$\mu\mathrm{m}^2$) when driven by an external magnetic field applied along the nanostrip axis. The resulting DW speed v_{exp} is reported in Figure 2.

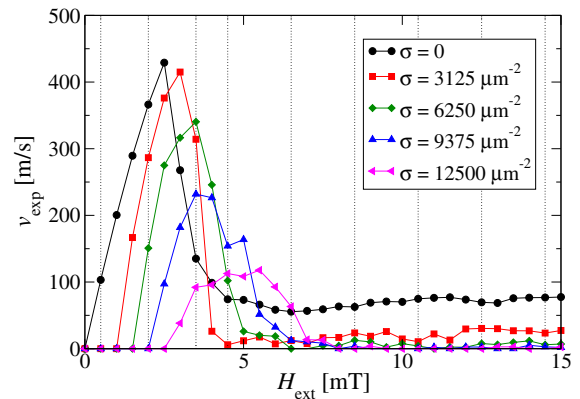At low fields, the void-free strip displays the well-know linear behavior up to the Walker breakdown H_W (about

Fig. 2. (Color online) The DW speed v_{exp} (see text for its definition) in the void-free and disordered nanostrips having different densities of void cells. Dotted vertical lines refer to the nine applied fields shown in Figure 1.

2.5 mT in this case), due to the undisturbed motion of the V-DW (first two rows of Fig. 1). On the contrary, in the disordered strips, the V-DW is set into motion only for fields larger than a depinning field $H_{\mathrm{dep}}(\sigma)$, which increases with σ, and reaching the maximum speed at lower values compared to the void-free case, as one can expect. This pinning is due to the collective contribution of the voids, and it is known as *collective pinning*. The highest speed results at a disorder-dependent Walker field $H_W(\sigma)$. The reason is due to progressive difficulty to nucleate an antivortex (AV-DW) with an upward-oriented core (white in the figures) from the bottom edge, whose retrograde motion is responsible for the steep drop in the speed in the void-free case. In the disordered strips, in fact, when the AV-DW enters the system, depending on the local void configuration, it can (i) be pushed back out of the system, i.e. it is immediately suppressed, (ii) find a "free channel", i.e. a path in the strip free of voids enabling both forward or backward motion, or (iii) get pinned by a local void
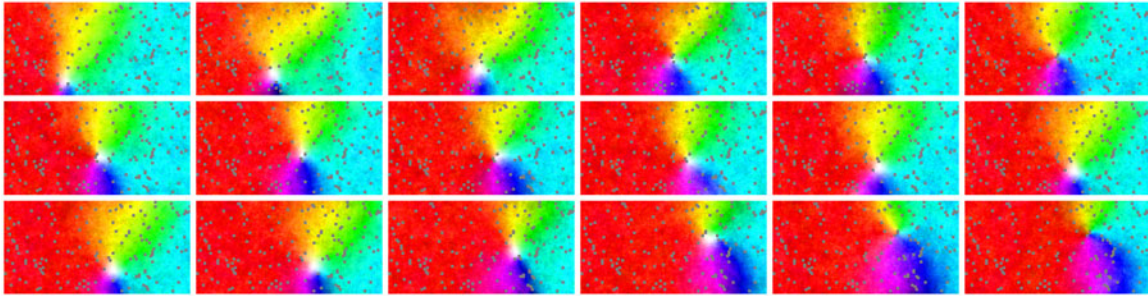
Fig. 3. (Color online) Dynamics of an antivortex DW driven by a field of 8.5 mT. The snapshots have sizes of 100×200 nm^2, and are shown every 0.1 ns, from top-left to bottom-right. Motion along a void-free channel (first three snapshots of the first and of the third row) can reach the remarkable velocity of about 200 m/s.

structure. The first case is similar to the suppression of the AV-DW nucleation in case of rough edges [15], while the other two are peculiar of our "bulk" disorder, and need a separate discussion (see below). As a consequence, the drop after the Walker breakdown is less deep, and more rounded, as in the limiting (and unrealistic) case of the highest void density. For fields higher than H_W, the increase of the pinning probability due to the *core pinning* mechanism (see below) leads to very low values of the experimental velocity. For instance, in Figure 1 at the highest field in the disordered strip a (rare) vortex DW is nucleated (bottom right), and indefinitely pinned by a local void configuration.

3.2 Dynamics of the antivortex DW

Figure 3, taken for $H = 8.5$ mT, helps us to better understand the richness of the AV dynamics moving between the edges of the nanostrip. The first row shows a nucleated and stable AV moving forward, in the direction of the field, along a small "channel" free of voids. The overall structure of the wall is highly deformed by the disorder, but still the central core moves at the remarkable speed of about 200 m/s. At the top of the core there are two groups of three adjacent voids each (let us call them "triplets" for short), to which the AV gets temporarily pinned. These triplets actually represent a barrier to the upward motion. Because of the high pressure of the external field, the AV is able to detach from them moving downward first, and then upward along another free channel. Finally, the wall reaches another triplet structure where it gets pinned indefinitely. This dynamics is quite typical at fields larger than $H_W(\sigma)$, even if occasionally the motion along free channels can be retrograde, as in the void-free case.

We do not actually know if the triplet structure induces a particular magnetic field distribution which acts as a natural pinning center for the AV-DW. We note that a triplet has a spatial extension (roughly 3 times the cell lateral dimension) which is close to the strip thickness of 10 nm. Clearly, further simulations varying the sample thickness and/or the void dimensions will confirm these conjectures. Anyway, we can at least conclude that some local structures of voids are able to control the DW dynamics of the AV-DW in an almost predictable way, even if we cannot supply further details.

The mechanism of pinning of the AV-DW is unique and can be dubbed as *core pinning*: the wall core stands exactly on a local structure of voids (another triplet, in the case of Fig. 3), and even the largest applied fields are not able to depin it. In fact, the Zeeman torque in the wall points out-of-plane (yellow-green and purple-blue regions), thus it is not directly pushing the central core. This torque thus induces demagnetizing fields, which actually try to push the wall away from the voids, but cannot compensate the reduction of the demagnetizing field due to a core with zero magnetization.

4 Current driven DW dynamics

4.1 Adiabatic spin-transfer torque effect

To investigate the effect of spin transfer torques, we apply a spin-polarized current with density $\mathbf{j} = -j_{\text{ext}}\hat{\mathbf{x}}$, and polarization $P = 0.5$ along strips of lengths 6.4 μm. Let us first consider the case of the adiabatic SST ($\xi = 0$ in Eq. (1)). As well-known, a threshold current exists (about 15 A/μm^2 here) below which there is no steady motion of the V-DW. This is referred as intrinsic pinning, and it is due to the balance between the adiabatic spin-torque and the effective field torques. The presence of the voids induces a significant distortion of the wall shape, leading to a more difficult balance of the two torques. The net effect is a *reduction* of the threshold critical current of almost 20%, as shown in Figure 4. This is quite a surprising result, as one expects in general an increasing difficulty of motion in case of a disordered system. We can also note that the lower threshold is independent of the void density, and resembles the typical rounding of a depinning transition at finite temperatures. Here, we must remind that we set the temperature to zero, and thus this rounding is only due to the presence of disorder.

At larger currents the highest speed is reached in the void-free strip, as expected. The DW dynamics is characterized by nucleation, forward motion, annihilation of an AV-DW, in both cases of void-free and disordered strips. Interestingly, the central core of the AV-DW is nucleated with an opposite out-of-plane magnetization compared to the field driven case. This is because of the opposite sign of the last term of equation (1) in respect of all the others. Surprisingly, we did not observe any core pinning, in contrast with the field-driven case. As the core shows the
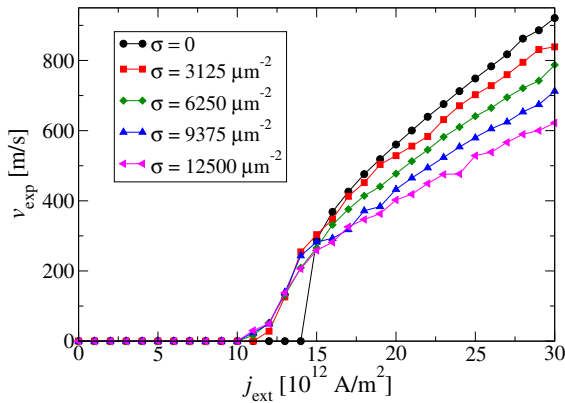
Fig. 4. (Color online) Experimental DW speed v_{exp} for spin-polarized currents j_{ext} and adiabatic spin-torque effects ($\xi = 0$ in Eq. (1)), in a void-free nanostrip ($\sigma = 0$, black dots), and in four disordered strips with different void densities.
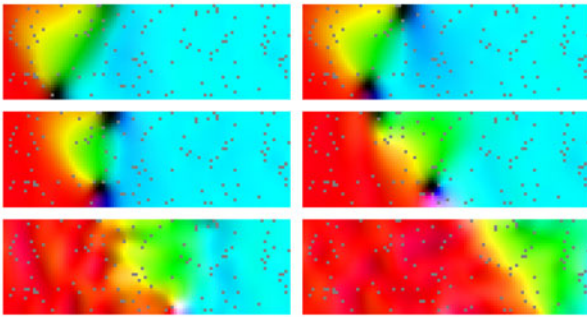

Fig. 5. (Color online) Dynamics of multiple antivortex in a strip with void density of 6250 μm^{-2}, with a spin-polarized current of 12 A/μm^2. The snapshots of 100×350 nm^2 are taken every 0.1 ns. The antivortex at the bottom edge is nucleated first and moves forward, while the second on the top edge nucleates later and moves backward. Their annihilation occurs within 0.5 ns.

largest magnetization gradients, the torque acting on it is always very large, and no void structure (at least in this case) is able to decrease the energy enough to stably pin the wall.

For relatively high void densities ($\sigma \geq 6250$ μm^{-2}), we also occasionally observe two different types of wall dynamics: (i) the nucleation of multiple AVs (Fig. 5), and (ii) the switching of polarity of the AV core (Fig. 6). A configuration with multiple AVs is highly unstable, as, in the case of Figure 5, they try to move in opposite directions. They quickly annihilate (less than 0.5 ns), anyway lowering the overall DW speed. On the contrary, the switch of the AV core, from upward (white) to downward (black) direction in Figure 6 does not lower the velocity significantly. The origin of this switch is not clear, by the way, as the local void does not show any particular structure, unless the voids in the bottom part of the strip could act as temporary barrier for the motion of the lower part of the AV (purple-blue region). Both these AV-DW dynamics occur especially for applied currents around the threshold value, which confirms the intrinsic instability of the magnetization dynamics in this region.
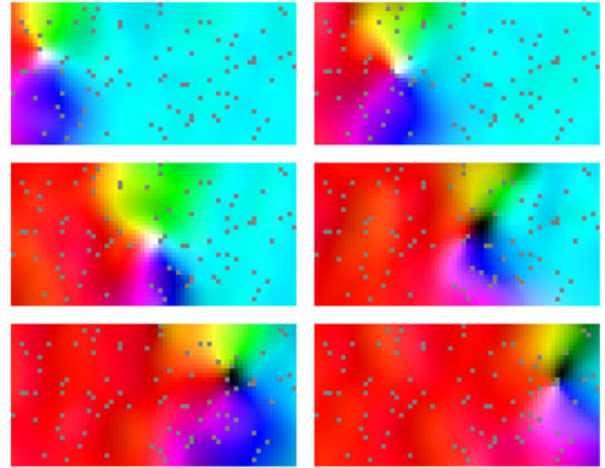

Fig. 6. (Color online) Switch of the core polarity of an antivortex during the forward motion in a strip with void density of 9375 μm^{-2}, under a spin-polarized current of 14 A/μm^2. The snapshots of 100×200 nm^2 are taken every 0.1 ns. The antivortex with upward/downward oriented core (white/back) moves downward/upward, respectively.

4.2 Non-adiabatic spin-transfer torque effect

We now consider the effect of the non-adiabatic SST on the DW dynamics, using a value of non-adiabaticity $\xi = 0.04$ in equation (1). The DW speed v_{exp} is reported in Figure 7, and shows Walker-like dynamics at low currents, and an adiabatic-like behavior at larger currents.

At low current values, no intrinsic pinning occurs, and the V-DW moves quite rigidly along the strip. In case of disordered strips, this happens for currents larger than a depinning current $j_{dep}(\sigma)$, in analogy with the field driven dynamics. Note that the depinning transition is rounded as in the case of thermal effects.

For large currents, an AV-DW is nucleated at current values which *increase* with the void densities. The maximum speeds thus occur at *more disordered* strips, and in the highest limits, the Walker breakdown is almost suppressed. This is an extremely unexpected but interesting result: the disorder acts to enhance the DW dynamics. For instance, at the void density $\sigma = 6250$ μm^2 there is no AV-DW nucleation, and the AV-DW moves forward with small deformations which accommodate for the void structure, but no pinning occurs. This is a quite different result in respect to the edge roughness effect [15], where the maximum speed is almost the same of the perfect strip: here, we have a significant increase of the highest attainable speed.

5 Discussion and conclusions

In this paper, we have extended our recent study of domain wall dynamics in disordered permalloy nanostrips [19]. The presence of disorder induces a rich variety of effects on the DW dynamics, including different DW pinning mechanisms (collective and core pinning), as well as
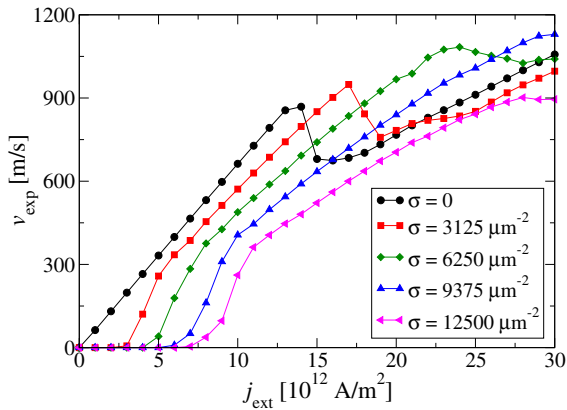
Fig. 7. (Color online) DW speed v_{exp} for spin-polarized currents j_{ext} and both adiabatic and non-adiabatic spin-torque effects ($\xi = 0.04$ in Eq. (1)), in a void-free nanostrip ($\sigma = 0$, black dots), and in four disordered strips.

partial suppression of both the Walker breakdown and the intrinsic pinning mechanism in the case of the adiabatic spin transfer torque. The presence or absence of these effects depends strongly on the mode of driving (field or current) as well as on the details of the DW structure (e.g. core pinning acts on the antivortex core). For mobile DWs the effect of disorder can be accounted for by describing it in terms of effective parameter values of the system (such as the effective damping parameter α), but this picture is complicated by the fact that DWs can also get pinned by the disorder.

As often mentioned, here we considered a zero temperature system, to better understand the effect of the structural disorder. In real systems one could also encounter creep motion consisting of a sequence of DW pinning and thermally activated depinning events. On the other hand, we have also seen that close to the depinning field/current density the velocity versus driving force relation can exhibit non-linearities typical of creep motion even for $T = 0$, thus highlighting the importance of being careful when interpreting the experimental velocity vs field/current density curves.

As any real system, including the ones used for various spintronics devices, necessarily includes several possible sources of structural disorder (e.g. thickness fluctuations of the strip, grain structure of the material, as well as various localized impurities and defects), the disorder effects for the DW dynamics need to be understood and controlled, in order to be able to produce devices operating in a reliable fashion. In particular, the inherently stochastic nature of the DW dynamics presents a challenge for devices where it is essential to control the DW dynamics in a reproducible manner. On the other hand, disorder can have also beneficial effects for technological applications: for instance, for $\xi > 0$ the DW velocity for a specific range of current densities can be increased when disorder is included or its strength is increased. At the same time the structural stability of the DW is enhanced by disorder (visible e.g. as the partial suppression of the Walker breakdown by the disorder, in combination with

a finite depinning field/current), suggesting that in some cases it could be desirable to deliberately engineer disorder into the system, for instance to replace notches to pin the DWs [14]. In addition, a related possibility is to control the material parameters of the system by doping, for instance by tuning the degree of non-adiabaticity of permalloy wires by doping them with vanadium [23].

References

1. S.P. Parkin, M. Hayashi, L. Thomas, Science **320**, 190 (2008)
2. D. Atkinson, D.S. Eastwood, L.K. Bogart, Appl. Phys. Lett. **92**, 022510 (2008)
3. J. He, S. Zhang, Appl. Phys. Lett. **90**, 142508 (2007)
4. T. Ono, Y. Nakatani, Appl. Phys. Express **1**, 061301 (2008)
5. E. Martinez, L. Torres, L. Lopez-Diaz, Phys. Rev. B **83**, 174444 (2011)
6. D.A. Allwood, G. Xiong, M.D. Cooke, C.C. Faulkner, D. Atkinson, N. Vernier, R.P. Cowburn, Science **296**, 2003 (2002)
7. P. Xu, K. Xia, C. Gu, L. Tang, H. Yang, J. Li, Nature Nanotechnol. **3**, 97 (2008)
8. E. Martinez, G. Finocchio, M. Carpentieri, Appl. Phys. Lett. **98**, 072507 (2011)
9. C.H. Marrows, G. Meier, J. Phys.: Condens. Matter **24**, 020301 (2012)
10. O. Boulle, G. Malinowski, M. Kläui, Mater. Sci. Eng. R **72**, 159 (2011)
11. G. Durin, S. Zapperi, *The Science of Hysteresis: Physical Modeling, Micromagnetics, and Magnetization Dynamics* (Academic Press, Amsterdam, 2006), Vol. II, Chap. III "The Barkhausen noise", pp. 181–267
12. T. Moore et al., J. Magn. Magn. Mater. **322**, 1347 (2009)
13. J. Akerman, M. Muñoz, M. Maicas, J.L. Prieto, Phys. Rev. B **82**, 064426 (2010)
14. M.A. Basith, S. McVitie, D. McGrouther, J.N. Chapman, Appl. Phys. Lett. **100**, 232402 (2012)
15. Y. Nakatani, A. Thiaville, J. Miltat, Nat. Mater. **2**, 521 (2003)
16. H. Min, R.D. McMichael, M.J. Donahue, J. Miltat, M.D. Stiles, Phys. Rev. Lett. **104**, 217201 (2010)
17. L. Laurson, A. Mughal, G. Durin, S. Zapperi, IEEE Trans. Magn. **46**, 262 (2010)
18. L. Laurson, C. Serpico, G. Durin, S. Zapperi, J. Appl. Phys. **109**, 07D345 (2011)
19. B. Van de Wiele, L. Laurson, G. Durin, Phys. Rev. B **86**, 144415 (2012)
20. S. Zhang, Z. Li, Phys. Rev. Lett. **93**, 127204 (2004)
21. A. Vansteenkiste, B. Van de Wiele, J. Magn. Magn. Mater. **323**, 2585 (2011)
22. B. Van de Wiele, F. Olyslager, L. Dupre, D. De Zutter, J. Magn. Magn. Mater. **322**, 469 (2010)
23. S. Lepadatu et al., Phys. Rev. B **81**, 020413 (2010)